Optimization of User Equipment Random Access Delay in LEO Satellite Communication Systems via Synchronization Signal Block Periodicity

A Thesis
Presented to
The Academic Faculty

by

Po-Yu Yen

In Partial Fulfillment
of the Requirements for the Degree
Master of Science in the
Graduate Institute of Communication Engineering

National Taiwan University

July 2025

ABSTRACT

Low Earth Orbit (LEO) satellite network has been a promising technology due to the wide spread coverage area and high data throughput. However, with the high speed of satellites, frequent handover is unavoidable for user equipments (UEs) on the ground, causing significant interruption time and signaling overhead. Thus, we introduce a quasi-earth-fixed satellite beam scheme to solve the continually handover from the UEs at the cell edge. In this scheme, we allocate the satellite beams to the ground cells in order to maximize overall throughput. After that, we also propose a UE cell selection algorithm, which base on both position information and UE measurement.

TABLE OF CONTENTS

LIST OF TABLES

LIST OF FIGURES

CHAPTER 1

INTRODUCTION

Non terrestrial network (NTN) has become a promising technique in next generation network. It provides network connectivity to area that traditional network platform cannot reach. For instance, forests, oceans, and deserts. Various platforms are used to provide network services in NTN, such as GEO, MEO, LEO satellites, UAVs, and drones. Among these platforms, LEO satellites are the most actively discussed. These satellites are located at altitude 500 to 2000 kilometers. The strongest advantage is that they provide global coverage, low latency, and high throughput compared to MEO or GEO satellites.

However, to acheive LEO satellite network service, there are some key challanges that need to be resolved. One of the challanges is the unavoidable frequent handover [1]. The high speed of LEO satellite forces user equipments (UEs) on the ground to switch the serving satellites frequently, as shown in Figure 1. In such scenario, the signalling overhead led by handover signals and the handover interruption time are big issues. 3GPP has discussed some solutions to deal with these issues. By using quasi-earth-fixed cell and satellite switch with resynchronization [2], the frequent handovers are avoided and the signalling overhead is reduced. For UEs that have already accessed to the network, they can receive the upcoming serving satellite information from the previous one. Also, with the help of the ephemeris data of satellies and the position information of UEs, the matching between satellites and UEs has been largely improved [3]. Nontheless, for those UEs who have not access to the network, the random access procedure is the only way for them to get into the network. To establish the connection between satellites and UEs, satellites need to transmit synchronization signal block (SSB) to ground for UEs to capture. Once UEs have successfully receive SSBs, the random access procedure starts and the UEs are able to access to the satellite network. Typically in terrestrial network, ground stations send SSB to the serving area every 20 milliseconds. However, the traditional SSB specifications in LEO satellite communication system do not work because the power budget in LEO satellite is so tight that the power is not enough to send all the serving cells in such a short periodicity. Thus, in this thesis we will find out how to deal with this issue by adjust the SSB periodicity and transmitted power.

Cell Diameter Size (km)	UE Speed (km/hr)	Satellite Speed (km/s)	Time to HO (s)
50 (lower bound)	+500	7.56 (NOTE 1)	6.49
	-500		6.74
	+1200		6.33
	- 1200		6.92
	Neglected		6.61
1000 (upper bound)	+500		129.89
	-500		134.75
	+1200		126.69
	- 1200		138.38
	Neglected		132.28

Figure 1: Time to handover for min/max cell diameter and varying UE speed

CHAPTER 2

BACKGROUND AND RELATED WORK

CHAPTER 3

SYSTEM MODEL

3.1 System Overview

This chapter introduces the considered LEO satellite communication system, as illustrated in Figure 2. The network consists of N satellites, denoted by $\mathcal{N} = \{n \mid n = 1, 2, \ldots, N\}$, where each satellite is equipped with M beams, represented by $\mathcal{M} = \{m \mid m = 1, 2, \ldots, M\}$. The coverage area is partitioned into K ground cells, $\mathcal{K} = \{k \mid k = 1, 2, \ldots, K\}$, and contains U user equipments (UEs), indexed by $\mathcal{U} = \{u \mid u = 1, 2, \ldots, U\}$.

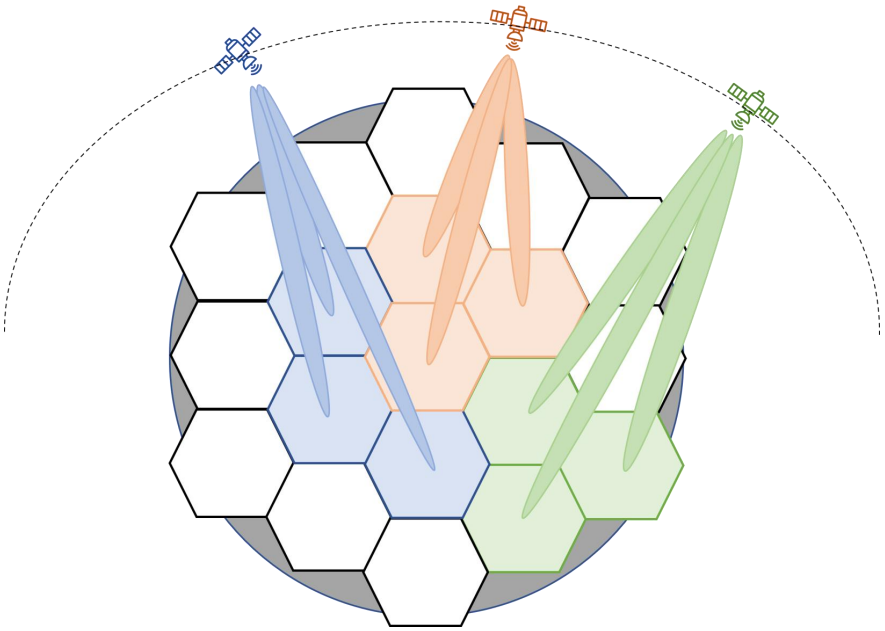

Figure 2: Illustration of satellite beams and cells.

In this thesis, we adopt the quasi-earth-fixed cell scheme. Unlike the earth-moving cell scheme—where the coverage areas of satellite beams move as the LEO satellites orbit—this approach directs satellite beams so that each beam consistently covers the same geographical cell for a given period. Thus, the coverage area of each satellite beam remains fixed relative to the ground during that interval. Throughout, we assume each satellite beam is oriented toward the center of its designated cell.

For each satellite, power allocation is subject to a total power budget. Let $P_{n,m}[t]$ denote the transmitted power of the m-th beam from the n-th satellite

at time slot t. The aggregate transmit power of all beams on any satellite must satisfy:

$$\sum_{m} P_{n,m}[t] \leq P_s, \quad \forall n \in \mathcal{N} \tag{3.1}$$

where P_s is the maximum transmit power per satellite.

To achieve optimal coverage and minimize overlap, all ground cells are arranged in a regular hexagonal grid, ensuring uniform cell size. Each cell is served by at most one satellite beam in any given time slot.

The locations of UEs wishing to access the network are assigned randomly within their corresponding cells, and the population of each cell are generated according to area population density statistics.

3.2 Channel Model

3.2.1 Free Space Path Loss

In the LEO satellite system, the free space path loss from satellite n to cell k is expressed as follows [4]:

$$L_{n,k} = \left(\frac{\lambda}{4\pi d_{n,k}}\right)^2 \tag{3.2}$$

where λ is the wavelength, and $d_{n,k}$ is the distance between the n-th satellite and the center of the k-th cell.

3.2.2 Shadowed-Rician Fading Channel

The shadowed-Rician fading model is suitable for satellite communication systems because it accurately reflects the physical propagation environment, capturing both the presence of a strong line-of-sight (LoS) signal and the effects of shadowing from obstacles [5]. Let $h_{n,k}$ denote the channel gain between the n-th satellite and the k-th cell. The cumulative distribution function (CDF) of the channel gain is:

$$F_{h_{n,k}}(x) = K \sum_{n=0}^{\infty} \frac{(m)_n \, \delta^n \, (2b)^{1+n}}{(n!)^2} \gamma\left(1+n, \frac{x}{2b}\right) \tag{3.3}$$

where $K = \left(\frac{2bm}{2bm+\Omega}\right)^m / 2b$, $\delta = \Omega/(2bm+\Omega)/2b$, Ω is the average power of the LoS component, $2b$ is the average power of the multipath component except the LoS component, and m is the Nakagami parameter.

3.2.3 Antenna Radiation Pattern

We introduce the antenna radiation pattern in [6]:

$$G(\theta_{n,m,u}) = G_{max}\left[\frac{J_1\left(\mu(\theta_{n,m,u})\right)}{2\mu(\theta_{n,m,u})} + 36\frac{J_3\left(\mu(\theta_{n,m,u})\right)}{\mu(\theta_{n,m,u})^3}\right]^2 \tag{3.4}$$

where $\theta_{n,m,u}$ is the boresight angle between the user position and the beam center with respect to the satellite, G_{max} is the maximum antenna gain, $\mu(\theta)$ is defined as $2.07123 \cdot \sin(\theta)/\sin(\theta_{3dB})$, θ_{3dB} is the 3 dB half-power beamwidth angle of the antenna, and $J_1(\cdot)$, $J_3(\cdot)$ are the Bessel functions of the first kind of orders 1 and 3, respectively.

With the transmitted power $P_{n,m}$ from the m-th beam of the n-th satellite, the received power at the u-th user, $\hat{P}_{n,m,u}$, is given by:

$$\hat{P}_{n,m,u} = P_{n,m} \cdot L_{n,k} \cdot h_{n,k} \cdot G(\theta_{n,m,u}) \tag{3.5}$$

where k is the cell where user u is located.

3.3 Synchronization Signal Block Model

This section describes the SSB periodicity settings based on 3GPP protocol and their impact on system operation. According to 3GPP protocol [3], the supported synchronization signal block (SSB) periodicity values are $\{20, 40, 80, 160\}$ milliseconds. The SSB periodicity of each cell is defined as:

$$T_k^{SSB} \in \{20, 40, 80, 160\}, \quad \forall k \in \mathcal{K} \tag{3.6}$$

The duration of each time slot is set to 160 ms. To simplify computational complexity, both the positions of satellites and UEs are assumed fixed within each time slot. The SSB periodicity specification for each cell remains unchanged throughout the slot.

Let $\Delta_{n,m}[t]$ denote the set of cells served by the m-th beam of the n-th satellite at time slot t. Since the time duration of each slot is 160 ms and the SSB periodicity is 20, 40, 80, or 160 ms, the number of elements in $\Delta_{n,m}[t]$ must be 0, 1, 2, 4, or 8, as shown in Figure 3.

T_k^{SSB}	$\lvert\Delta\rvert$	Cell Pattern k							
20	1	1	1	1	1	1	1	1	1
40	2	1	2	1	2	1	2	1	2
80	4	1	2	3	4	1	2	3	4
160	8	1	2	3	4	5	6	7	8
		20ms	20ms	20ms	20ms	20ms	20ms	20ms	20ms

Figure 3: Illustration of SSB periodicity and cell patterns for different periodicity settings.

3.4 UE Random Access Delay

The random access delay T_u for the u-th UE is defined as the time duration between the start of SSB measurement and the successful reception of SSB, as

shown in Figure 4. T_u can be decomposed into two parts: T_u^i (initial waiting time) and T_u^l (additional delay due to failed attempts). T_u^i is the time from the start of SSB measurement to the arrival of the first SSB, and T_u^l is the time from the first SSB arrival to the successful SSB reception.

Since the UE can start SSB measurement at any time, T_u^i is a uniformly distributed random variable $U(0, T_{k_u}^{SSB})$. T_u^l is a multiple of $T_{k_u}^{SSB}$, depending on the number of failures Q_u. If the received SSB power $\hat{P}_{n,m,u}$ is less than the threshold P_{th}, the UE fails to measure SSB. The probability that the received SSB power is less than P^{th} is denoted as P_u^0. The mathematical formulation is as follows:

$$T_u = T_u^i + T_u^l \tag{3.7}$$

$$F_{T_u^i}(t) = \begin{cases} \frac{t}{T_{k_u}^{SSB}}, & 0 \le t < T_{k_u}^{SSB} \\ 1, & t \ge T_{k_u}^{SSB} \\ 0, & \text{otherwise} \end{cases} \tag{3.8}$$

$$T_u^l = Q_u \cdot T_{k_u}^{SSB} \tag{3.9}$$

$$\Pr\left[Q_u = n\right] = (1 - P_u^0)(P_u^0)^n \tag{3.10}$$

where k_u is the cell where the u-th UE is located.

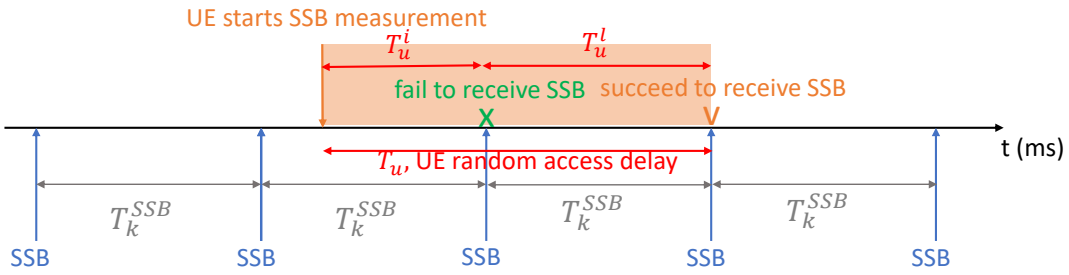

Figure 4: Illustration of UE random access delay. T_u is decomposed into T_u^i (initial waiting time) and T_u^l (additional delay due to failed attempts).

3.5 Problem Formulation

This section formulates the optimization problem based on recent 3GPP standardization discussions. In the 3GPP RAN1 #116 meeting [7], further specifications for the LEO satellite communication scenario were defined. The main challenge is to provide random access to a large number of cells with limited satellite power. Extending the SSB periodicity for some cells reduces satellite power consumption but increases UE random access delay. The transmitted SSB power also affects the success probability of the random access procedure. The trade-off

among power allocation, SSB periodicity, and UE random access delay is modeled as follows:

$$\min_{\Delta, P_{n,m}} \sum_{u \in \mathcal{U}} T_u$$

subject to

$$\begin{aligned} &\sum_{m} P_{n,m}[t] \leq P_s, \quad \forall n \in \mathcal{N} \\ &|\Delta_{n,m}[t]| \in \{0, 1, 2, 4, 8\}, \quad \forall n \in \mathcal{N}, m \in \mathcal{M} \\ &\Delta_{n,m}[t] \cap \Delta_{n',m'}[t] = \emptyset, \quad \forall n, n' \in \mathcal{N}, m, m' \in \mathcal{M}, (n,m) \neq (n',m') \end{aligned} \tag{3.11}$$

CHAPTER 4

PROPOSED ALGORITHM

CHAPTER 5

PERFORMANCE EVALUATION

All figures should be of the same width whenever possible for consistency.

5.1 Simulation Setup

We use BONMON [**?**] to solve the optimization problem. The simulation setup follows that in [**?**].

5.2 Simulation Results

CHAPTER 6

CONCLUSION AND FUTURE WORK

REFERENCES

[1] "Solutions for nr to support non-terrestrial networks (ntn)," 3rd Generation Partnership Project (3GPP), Technical Report TR 38.821, 2023, release 16. Online Available at: https://www.3gpp.org/dynareport/38821.htm

[2] "Nr; nr and ng-ran overall description; stage-2," 3rd Generation Partnership Project (3GPP), Technical Specification TS 38.300, 2024, release 18. Online Available at: https://www.3gpp.org/dynareport/38300.htm

[3] 3GPP, "Radio Resource Control (RRC) protocol specification," 3rd Generation Partnership Project (3GPP), Technical Report TR 38.331, March 2024, version 18.1.0. Online Available at: https://www.3gpp.org/ftp/Specs/archive/38_series/38.331/

[4] J. Wang, C. Jiang, L. Kuang, and R. Han, "Satellite multi-beam collaborative scheduling in satellite aviation communications," *IEEE Transactions on Wireless Communications*, vol. 23, no. 3, pp. 2097–2111, 2024.

[5] D.-H. Jung, J.-G. Ryu, W.-J. Byun, and J. Choi, "Performance analysis of satellite communication system under the shadowed-rician fading: A stochastic geometry approach," *IEEE Transactions on Communications*, vol. 70, no. 4, pp. 2707–2721, 2022.

[6] S.-H. Chen, L.-H. Shen, K.-T. Feng, L.-L. Yang, and J.-M. Wu, "Energy-efficient joint handover and beam switching scheme for multi-leo networks," in *2024 IEEE 99th Vehicular Technology Conference (VTC2024-Spring)*, 2024, pp. 1–7.

[7] 3GPP TSG RAN WG1, "Final report of 3gpp tsg ran wg1 #116 v1.0.0," 3rd Generation Partnership Project (3GPP), Athens, Greece, Technical Report R1-2400000, February 2024, meeting held February 26th – March 1st, 2024. Online Available at: https://www.3gpp.org/ftp/tsg_ran/WG1_RL1/TSGR1_116/Report/Final_Report_3GPP_TSG_RAN_WG1_116_v1.0.0.pdf